Integration of the classical equations of motion on ab initio molecular potential energy surfaces using gradients and Hessians: application to translational energy release upon fragmentation

Trygve Helgaker, Einar Uggerud
Department of Chemistry, University of Oslo, P.O. Box 1033 Blindern, N-0315 Oslo 3, Norway

and

Hans Jørgen Aa. Jensen
Department of Chemistry, Århus University, DK-8000 Aarhus C, Denmark

Received 8 June 1990; in final form 16 June 1990

A new method for calculating classical trajectories on molecular ab initio potential energy surfaces is presented. The equations of motion are integrated on a sequence of model surfaces constructed from analytically calculated molecular gradients and Hessians. The method avoids the explicit calculation of the total surface and is therefore applicable whenever the gradient and Hessian can be calculated. The method is applied to the unimolecular fragmentations of H_3 and CH_2OH^+, yielding the translational energy released upon separation of the products.

1. Introduction

The calculation of the trajectories traversed by the individual atoms of a molecular system requires a precise knowledge of the potential energy surface. Accurate surfaces may be obtained from ab initio electronic structure calculations [1]. The traditional approach is to calculate the energy for a large number of geometrical configurations and to fit an analytical function to these energies. The dynamical problem is then solved by integrating the equations of motion numerically on this function, using for example the Runge–Kutta method [2]. The bottleneck in this procedure is the construction of the surface. The high dimensionality of most surfaces makes it necessary to introduce a number of assumptions, the validity of which may be questionable. Also, the fitting procedure itself is not without problems.

In this paper we present an alternative scheme which avoids the explicit calculation of the molecular surface. Instead a sequence of local approximations to the true surface is constructed along the classical trajectory. The local surfaces are calculated as needed in the course of the integration and only those parts of the surface actually traversed by the molecule are therefore considered. This makes the method applicable to larger systems without having to introduce arbitrary assumptions.

The implementation of this scheme depends on the nature of the local model surfaces. We use surfaces constructed from second-order Taylor expansions of the ab initio surface. The advent of efficient methods for calculating analytical molecular gradients and Hessians from ab initio wave functions has made this scheme practicable [3]. Gradients and Hessians may now be calculated at a reasonable cost for most wave functions, in particular, multiconfigurational self-consistent field (MCSCF) functions. Such wave functions are usually needed for the proper description of bond breaking and formation.

To illustrate the method we present calculations on the fragmentation processes of H_3 and protonated

0009-2614/90/$ 03.50

formaldehyde CH_2OH^+. The calculations give interesting snapshots of the processes and allow us to estimate the relative translational energy released upon elimination of H_2, observable in mass spectrometric experiments.

2. Trust-region dynamics

As noted above, at a given point on the trajectory we make a second-order model of the true ab initio surface and carry out the integration on this model. The model is a good approximation to the true surface only in a small region around the expansion point, *the trust region*. The calculated trajectory is therefore not allowed to leave this region. Inside the trust region, the integration is trivial since the second-order model trajectory may be expressed in a closed analytical form. In the following we first derive expressions for the model trajectory and then discuss the size of the trust region (the trust radius). The trust region and the model surface are concepts borrowed from optimization theory [4].

In Cartesian coordinates the classical equations of motion of an N-particle system are given by

$$m\ddot{x} = -\frac{\mathrm{d}V(x)}{\mathrm{d}x} . \tag{1}$$

Here x is a vector containing the $3N$ Cartesian coordinates, $V(x)$ is the potential energy of the system, and m is a $3N$-dimensional diagonal matrix containing the N nuclear masses m_i,

$$m = \mathrm{diag}(m_1, m_1, m_1, m_2, m_2, m_2, m_3, \ldots, m_N) . \tag{2}$$

The model surface is obtained by expanding the potential to second order in the displacements

$$\Delta x = x - x^0 \tag{3}$$

around the reference geometry x^0,

$$V_{\mathrm{model}}(x) = V^0 + \tilde{G}\,\Delta x + \tfrac{1}{2}\Delta\tilde{x}\,H\,\Delta x . \tag{4}$$

Here V^0 is the potential energy at the expansion point and G and H its gradient and Hessian at this point. The equations of motion may now be written

$$m\,\Delta\ddot{x} = -G - H\,\Delta x . \tag{5}$$

We now introduce normal coordinates Q in the usual way by diagonalizing the mass-weighted Hessian matrix,

$$Q = \tilde{L} m^{1/2}\,\Delta x , \tag{6}$$

$$g = \tilde{L} m^{-1/2} G , \tag{7}$$

$$\omega^2 = \tilde{L} m^{-1/2} H m^{-1/2} L . \tag{8}$$

Here g and ω^2 are the gradient and Hessian in normal coordinates. The elements of the diagonal Hessian may be positive, negative, or zero. The corresponding elements of the diagonal matrix ω (the frequencies) are then real, imaginary, or zero. The conjugate momenta P are related to the Cartesian momenta p as

$$P = \tilde{L} m^{-1/2} p . \tag{9}$$

The equations of motion are now separated and may be written

$$\ddot{Q}_i = -g_i - \omega_i^2 Q_i . \tag{10}$$

Solving these equations with the initial conditions

$$Q_i = 0 , \tag{11}$$

$$P_i = P_i^0 , \tag{12}$$

we obtain

$$Q_i(t) = \frac{P_i^0}{\omega_i}\sin(\omega_i t) - \frac{g_i}{\omega_i^2}\left[1 - \cos(\omega_i t)\right] , \tag{13}$$

$$P_i(t) = P_i^0 \cos(\omega_i t) - \frac{g_i}{\omega_i}\sin(\omega_i t) . \tag{14}$$

In the special case of zero frequency these equations take the form

$$Q_i(t) = P_i^0 t - \tfrac{1}{2} g_i t^2 , \tag{15}$$

$$P_i(t) = P_i^0 - g_i t \tag{16}$$

and when the frequency is imaginary the solution may be written in terms of the hyperbolic functions

$$Q_i(t) = \frac{P_i^0}{|\omega_i|}\sinh(|\omega_i| t) + \frac{g_i}{|\omega_i|^2}\left[1 - \cosh(|\omega_i| t)\right] , \tag{17}$$

$$P_i(t) = P_i^0 \cosh(|\omega_i| t) - \frac{g_i}{|\omega_i|}\sinh(|\omega_i| t) . \tag{18}$$

Once $Q(t)$ and $P(t)$ have been obtained from the above expressions the Cartesian coordinates and momenta are calculated as

$$x = x^0 + m^{-1/2} LQ , \quad (19)$$

$$p = m^{1/2} LP . \quad (20)$$

The calculation of the trajectory on a second-order surface is therefore trivial once the gradient and Hessian are available.

The integration of the complete trajectory proceeds in steps. We start by calculating the electronic energy, gradient, and Hessian at the initial point. This defines the local model surface. The integration is carried out to the boundary of the trust region, and the final point of this trajectory becomes the initial point for the local trajectory in the next iteration. The energy, gradient, and Hessian are recalculated, a new model surface constructed and a new local trajectory calculated. This process is repeated until the trajectory is complete.

In the first iteration a small trust radius of 0.01 atomic units is used. This is updated in subsequent iterations by the usual feedback mechanism of trust-region optimization [4]. The change in potential energy estimated from the second-order surface is compared with the true energy calculated in the next iteration. The trust radius is increased or reduced based on this comparison. It may, however, happen that large contributions from the individual modes result in a small overall change in the energy. In such cases the predicted energy cannot be used for updating the trust region.

In the course of the integration the anharmonicity of the potential surface is estimated by comparing the Hessians at adjacent points. In choosing the next step, the estimated anharmonic contribution to the energy of each mode is not allowed to exceed 1% of the harmonic contribution. The accuracy of the integration may be monitored by comparing the total kinetic energies as calculated from the integrated momenta and from the conservation of energy. In the calculations on H_3 and CH_2OH^+ below, these never differ by more than 0.8% and 0.7%, respectively, and at the end of the integrations by only 0.2% and 0.1%. This indicates that the calculated trajectories are close to the exact.

3. Calculations

To illustrate the method we calculate the relative translational energies released during the eliminations of H_2 from H_3 and CH_2OH^+. The translational energy released upon fragmentation of metastable CH_2OH^+ ions has been measured by mass spectrometric methods [5], and it is known that the ions possess no excess kinetic energy in the transition state [6]. The reactive trajectories therefore pass through the saddle point with practically no velocity. This simplifies the calculation since the initial conditions are well defined. To simplify further, we ignore zero-point vibrations, reducing the calculation to one trajectory for each system.

In the calculations on H_3 we use van Duijneveldt's 4s basis contracted to 2s with one set of p functions (exponent 0.75) added [7]. The wave function is constructed by distributing the electrons among the three most important σ orbitals in all possible ways (complete active space MCSCF). The calculations were carried out using the SIRIUS/ABACUS program system [8,9]. The gradient and Hessian are calculated analytically to an accuracy of 10^{-8} in each iteration. Details about the transition state and fragments are given in tables 1 and 2. The theoretical

Table 1
Energy, geometry, population analysis [a], and harmonic frequencies of H_3 at the transition state

energy (au)	−1.620426
R_{HH} (Å)	0.958
$\delta_{H(terminal)}$ [a] (e)	−0.017
$\delta_{H(middle)}$ (e)	0.034
$\nu_1\,\sigma_g^+$ (cm^{-1})	1933
$\nu_2\,\sigma_u^+$ (cm^{-1})	2185i
$\nu_3\,\pi_u$ (cm^{-1})	928

[a] We use Ciolowski's population-analysis-based dipole gradients [10]. δ are the atomic net polulations.

Table 2
Energies, geometry, and harmonic frequency of H_3 dissociation fragments

energy (H) (au)	−0.497726
energy (H_2) (au)	−1.149618
R_{HH} (Å)	0.756
$\nu_1\,\sigma_g^+$ (cm^{-1})	4277

barrier height is 71 kJ/mol. Harmonic zero-point vibrations reduce the barrier to 68 kJ/mol. This is significantly higher than the theoretical value 41 kJ/mol obtained by Siegbahn and Liu [11]. However, the wave function is adequate for our purposes.

The fragmentation is initiated at the rotation- and vibration-less transition state by adding a small momentum to the reaction mode. The trajectory is then integrated to complete dissociation, see fig. 1 and table 3. The separation between the centers of mass increases from 1.44 Å at the transition state to 3.57 Å at the point of maximum velocity (14.1 km/s) in 35.9 fs. There is then a slight retardation because of a small attractive but nonphysical force arising from the use of a finite orbital basis (basis-set superposition). The energy released as translation is 66.7 kJ/mol, i.e. 94% of the barrier. Hence nearly all of the energy is converted to relative translation. Sixty-seven iterations are required to reach this point. The separation increases on average by 0.03 Å in each iteration, the average time step is 0.5 fs.

During the fragmentation process, the H_2 molecule acquires 6% of the released energy (345 cm^{-1}) as vibrational. The frequency is found to be about 4270 cm^{-1}, just below the harmonic frequency calculated at the same level (4277 cm^{-1}). This is to be expected since very little energy has been transferred to this mode.

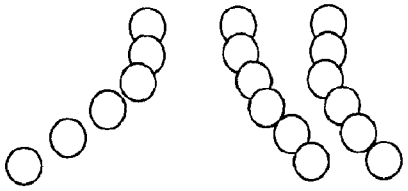

Fig. 1. The dissociation of H_3 at six different times, see table 3. The coordinate system is shifted downwards with time.

Table 4
Energies, geometries [a], population analysis [10] and harmonic frequencies of CH_2OH^+

	Equilibrium	Transition state
energy (au)	−114.059634	−113.887090
R_{CO} (Å)	1.229	1.184
R_{CH_A} (Å)	1.078	1.087
R_{CH_B} (Å)	1.080	1.225
R_{OH_C} (Å)	0.960	1.377
$\angle OCH_A$ (deg)	116.4	134.0
$\angle OCH_B$ (deg)	121.7	116.2
$\angle COH_C$ (deg)	117.8	58.7
δ_C [b] (e)	0.83	0.74
δ_O (e)	−0.62	−0.52
δ_{H_A} (e)	0.15	0.21
δ_{H_B} (e)	0.14	0.00
δ_{H_C} (e)	0.50	0.58
ν_1 a' (cm^{-1})	3958	3287
ν_2 (cm^{-1})	3428	2485
ν_3 (cm^{-1})	3280	2284
ν_4 (cm^{-1})	1832	2052
ν_5 (cm^{-1})	1591	1658
ν_6 (cm^{-1})	1483	1300
ν_7 (cm^{-1})	1190	2434i
ν_8 a'' (cm^{-1})	1380	1192
ν_9 (cm^{-1})	1058	160

[a] Numbering of atoms as in fig. 2. [b] Atomic net population.

The fragmentation of protonated formaldehyde is calculated at the Hartree–Fock level using the 4-31G** basis [12] [#1]. The equilibrium- and transition-state species are listed in table 4, the fragments in table 5. The theoretical barrier height is 277 kJ/mol (288 when corrected for zero-point vibrations).

[#1] Polarization exponents are 0.8 on carbon and oxygen, 1.1 on hydrogen.

Table 3
Details of H_3 dissociation trajectory. See fig. 1

Iteration	Time (fs)	Separation between centers of mass (Å)	Electronic energy (au)	Translational energy (au)
0	0.0	1.437	−1.620426	1.25×10^{-9}
4	14.7	1.453	−1.620641	0.0000602
24	20.1	1.596	−1.626824	0.0046887
34	25.1	2.078	−1.639863	0.0193085
46	29.9	2.719	−1.645508	0.0246581
61	34.9	3.422	−1.647240	0.0254001

Table 5
Energies, geometries, population analysis [10] and harmonic frequencies of CH_2OH^+ dissociation fragments

energy (HCO^+) (au)	−112.861233
R_{CO} (Å)	1.086
R_{CH} (Å)	1.086
δ_C [a] (e)	0.78
δ_O (e)	−0.16
δ_H (e)	0.39
$\nu_1\,\sigma^+$ (cm^{-1})	3414
ν_2 (cm^{-1})	2498
$\nu_3\,\pi$ (cm^{-1})	984
energy (H_2) (au)	−1.131334
R_{HH} (Å)	0.733
$\nu_1\,\sigma_g^+$ (cm^{-1})	4635

[a] Atomic net population.

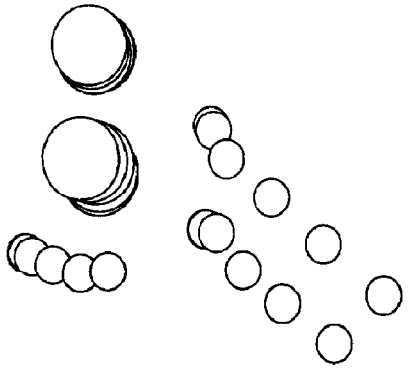

Fig. 2. Elimination of H_2 from CH_2OH^+. Geometries at six different times (see table 6) superimposed on each other, transition state at the bottom. The numbering of hydrogen atoms is H_A, H_B, and H_C counterclockwise starting in the lower left corner. Oxygen atom on top, carbon in middle. A rotating H_2 molecule leaves in the lower right corner. The linear bend of the remaining CHO^+ fragment is excited.

The experimental barrier is 218 kJ/mol [6]. The calculated trajectory is illustrated in fig. 2, see also table 6.

Maximum velocity of 15.6 km/s is reached after 35.4 fs at a separation of 3.62 Å. After this there is a slight retardation because of the incomplete basis. The translational energy is 230 kJ/mol, i.e. 83% of the released energy (zero-point vibrations disregarded). The vibrational energy released during the fragmentation mostly enters the linear bend of HCO^+, see fig. 2. We also note that in the process, H_2 acquires some rotational energy.

The observed translational energy is 64% of the experimental barrier height [5]. Our calculation significantly overestimates this value. We suspect that the neglect of zero-point vibrations is the most important source of error. Preliminary calculations on the deuterated (CD_2OD^+) and undeuterated (CH_2OH^+) species without including zero-point vibrations give almost identical translational energies at the 4-31G level, whereas experiments suggest that the relative translational energy increases significantly (from 64% to 73%) upon deuteration [5]. Since zero-point vibrations are less important for the deuterated species, these findings indicate that zero-point vibrations are effective in trapping the energy released during the fragmentation. We will investigate the importance of zero-point vibrations as well as barrier tunneling in a forthcoming paper.

A more accurate electronic wave function will certainly affect the calculated relative translational energy. We note, however, that the transition state of the wave function obtained by distributing eight electrons among eight orbitals is close to the transition state at the Hartree–Fock level. Large changes in the relative amounts of translational and vibra-

Table 6
Details of CH_2OH^+ dissociation trajectory. See fig. 2

Iteration	Time (fs)	Separation between centers of mass (Å)	Electronic energy (au)	Translational energy (au)
0	0.0	1.340	−113.887090	2.21×10^{-9}
5	14.7	1.363	−113.887894	0.000369
25	20.1	1.547	−113.913294	0.017779
40	24.9	2.043	−113.959632	0.060582
70	30.0	2.785	−113.990771	0.084122
103	35.0	3.555	−113.984215	0.087756

tional energies are therefore not expected for correlated wave functions.

It is interesting to note that for both H_3 and CH_2OH^+, the relative amount of energy converted to translation is smaller at the start of the trajectory than at the end. In the case of H_3, only 25% is converted to relative translation in the transition-state region. (Note that the reaction mode is not in the direction of relative translation.) At the end of the process as much as 94% of the energy has been converted. For protonated formaldehyde the corresponding numbers are 44% and 83%. It therefore appears impossible to estimate the translational energy release from a consideration of the transition state alone.

As a curiosity we note that the relative velocities are almost the same in both cases (14.1 and 15.6 km/s) so that both processes occur in about 35 fs. The reason is that the ratio between the reduced masses of the two systems roughly matches the ratio between their barrier heights.

4. Conclusions

We have demonstrated that it is possible to carry out classical trajectory calculations on ab initio potential energy surfaces without constructing the full surface in advance. This is significant since for larger systems the dimensionality of the surface makes the preliminary calculation of the surface impossible. A disadvantage of the method is the high cost of each trajectory. The large number of trajectories needed in many dynamical studies may therefore become prohibitively expensive. This problem is less severe for reactions starting at the transition state, since the initial conditions are then better defined. Frost and Smith [13] have proposed a scheme in which quasiclassical calculations are started in the transition-state region rather than with the reagents separated, bringing the number of trajetories needed for averaging down to a few hundred. Still, a large number of Hessian calculations would be needed for quasiclassical dynamics, making the proposed method costly. This should, however, be contrasted with the impossibility of constructing in advance many-dimensional ab initio surfaces for systems containing more than a few atoms.

Very recently a paper by Gibson and Scheraga [14] appeared in which they propose a similar scheme for molecular-dynamics simulations of peptides. These authors use a third-order expansion of an empirical energy surface. For ab initio surfaces third-order expansions are not yet feasible and the second-order scheme presented above appears to be the only practical approach. The cost of our method scales as the cost of the electronic wave function, and it therefore becomes possible to carry out trajectory calculations on systems containing as many as ten atoms without making arbitrary assumptions about the energy surface.

Acknowledgement

This work was supported by VISTA (Statoil and the Norwegian Academy of Science and Letters) and the Carlsberg Foundation (Grant No. 88-0217/20). The calculations were performed under a grant of computer time provided by the Norwegian Academy of Science and Letters (Grant No. D.96.30.011).

References

[1] K.P. Lawley, I. Prigogine and S.A. Rice, eds., Ab initio methods in quantum chemistry, Advances in chemical, physics, Vols. 67, 69 (Wiley, New York, 1987).
[2] R.N. Porter and L.M. Raff, in: Dynamics of molecular collisions, Part B, ed. W.H. Miller (Plenum Press, New York, 1976).
[3] T. Helgaker and P. Jørgensen, Advan. Quantum Chem. 19 (1988) 183.
[4] R. Fletcher, Practical methods of optimization, Vol. 1 (Wiley, New York, 1980);
J.E. Dennis Jr. and R.B. Schnabel, Numerical methods for unconstrained optimization and nonlinear equations (Prentice-Hall, Englewood Cliffs, 1983).
[5] G. Hvistendahl and E. Uggerud, Org. Mass Spectrom. 20 (1985) 541, and references therein.
[6] G. Hvistendahl and E. Uggerud, Org. Mass Spectrom., submitted for publication.
[7] F.B. van Duijneveldt, IBM Res. Rept. RJ 945 (1971).
[8] H.J.Aa. Jensen and H. Ågren, Chem. Phys. 104 (1986) 229.
[9] T.U. Helgaker, J. Almlöf, H.J.Aa. Jensen and P. Jørgensen, J. Chem. Phys. 84 (1986) 6266.
[10] J. Cioslowski, J. Am. Chem. Soc. 111 (1989) 8333.
[11] P. Siegbahn and B. Liu, J. Chem. Phys. 68 (1978) 2457.
[12] R. Ditchfield, W.J. Hehre and J.A. Pople, J. Chem. Phys. 54, 724 (1971).
[13] R.J. Frost and I.W.M. Smith, Chem. Phys. 117 (1987) 421.
[14] K.D. Gibson and H.A. Scheraga, J. Comput. Chem. 11 (1990) 468.